Upconverting nanoparticles for cellular imaging

D. K. Chatterjee[*], E. Zhang[*] and Y. Zhang[*,#]

[*] Division of Bioengineering, National University of Singapore,
Singapore 117576, dev@nus.edu.sg
[#] Nanoscience and Nanotechnology Initiative, National University of Singapore,
Singapore 117576, biezy@nus.edu.sg

ABSTRACT

Fluorescent labels that are excited by the near infrared (NIR) radiation are advantageous because these give rise to minimal autofluorescence because of lack of efficient endogenous absorbers in the NIR spectral range [1-3], and results in very high signal to background ratios. Furthermore, photo-damage to cells and tissues is also greatly reduced because NIR is generally harmless to biomolecules in low doses. In this report we present the use of ultrafine, pure cubic silica coated $NaYF_4$ nanocrystals co-doped with lanthanide ions ions Yb^{3+} and Er^{3+}. To the best of our knowledge these represent the first report of the use of sub-40 nm upconversion nanoparticles in biomedical imaging.

Keywords: nanoparticles, imaging, lanthanides, upconversion

1 INTRODUCTION

Upconverting nanoparticles (UCN) are modified nanometer-sized composites which generate higher energy light from lower energy radiation, through the use of transition metal, lanthanide, or actinide ions doped into a solid-state host (Boyer, Vetrone et al. 2006). UCN have been used in immunohistochemistry [4], various in vitro assays [5, 6] and imaging in C. elegans [7].

We have reported UCN as imaging probes in live cells in vitro [8, 9]. There we demonstrated the use of PEI coated NaYF nanoparticles in targeted imaging of cancer cells. However, while fluorescent imaging with these nanoparticulate probes showed high signal to noise ratio and strong resistance to photobleaching, these were about 60nm in diameter. This makes them unsuitable for in vivo use. Also, high positive surface charge due to presence of PEI caused strong propensity for non-specific binding to cell surface/.

In this report, we present the synthesis, characterization and application of a new class of sub-40nm UCN as fluorescent molecular markers in vitro and in vivo. The nanoparticle has a core of sodium yttrium fluoride ($NaYF_4$) nanocrystals co-doped with the rare earth ions ytterbium (Yb^{3+}) and erbium (Er^{3+}). This is covered by a silica coat that not only makes the non-polar core soluble in polar physiologic salt solutions, but also helps the attachment of ligands that help to target the nanoparticles to molecular targets.

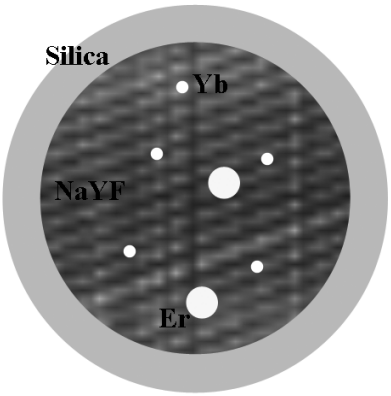

Figure 1: Schematic of the nanoparticle structure: Yb and Er doped in a NaYF crystalline matrix.

2 MATERIALS AND METHODS

2.1 Materials

FA (approximately 98%), dimethyl sulfoxide (DMSO), N-hydroxy-succinimide (NHS), 1-ethyl-3-(3-dimethyl-aminopropyl)carbodiimide (EDC), 3-mercaptopropionic acid (3-MPA), zinc phthalocyanine boric acid and sodium azide (99.99+%), sodium chloride (NaCl, >= 99.0%), yttrium chloride hexahydrate (YCl3•6H2O, 99.99%), ytterbium oxide (Yb2O3, 99.99%), erbium oxide (Er2O3, 99.99+%), ammonium fluoride (NH4F, 98+%), were purchased from Sigma-Aldrich. All of the reagents were used as received without further purification. YCl3 and NaCl stock solutions (0.2 M) were prepared by dissolving YCl3•6H2O and NaCl respectively in DI water. YbCl3 and

ErCl3 stock solutions (0.2 M) were prepared by dissolving corresponding oxides in hydrochloric acid.

HT29 cells (human colon adenocarcinoma cells) were cultured in a media constituted of DMEM, FBS and antibiotics (streptomycin and penicillin) in a ratio of 100:10:1 in 75 cm2 flasks. The cells were incubated in a 100% humidified incubator with 5% CO2 at 37°C. The cells were maintained using protocol as described before.

2.2 Characterization of the UCN

Transmission Electron Microscopy: The size and appearance of the nanoparticles were examined by transmission electron microscope (TEM). The silica/$NaYF_4$:Er^{3+},Yb^{3+} solution (4mM dispersed in ethanol) was immersed in an ultrasonic water bath (Elmasonic E60H) for sonication for 1 hour. 50µl of the NP solution was aspirated using a pipette and dropped onto a copper mesh placed on a piece of tissue paper. The dried copper mesh was loaded into the TEM for imaging.

Particle Analyzer: Silica/NaYF4:Er^{3+}, Yb^{3+} nanoparticles were dispersed in water (20mM) and kept in a 15ml test tube. The nanoparticles were mixed thoroughly using Vortex Mixer (Vision Scientific) until no precipitate was visible. The solution was further sonicated for 30 minutes in ultrasonic water bath (Elmasonic E60H). 800µlof the nanoparticle solution was aspirated using a pipette and filled into a folded capillary cell (DTS1060, Malvern Instrument), which was then loaded into the Zetasizer Nano Series (Nano-ZS, Malvern Instruments). Standard Operation Procedure (SOP) was created. Size and zeta potential were measured.

Emission Fluorescence: Square cuvette was filled with 3ml of silica/NaYF4:Er^{3+}, Yb^{3+} NP solution (20mM) and placed into the chamber of SpectraPro 2300i (0.300m Imaging Triple Grating Monochromator/Spectrograph, Acton Research Corporation). 980nm IR laser produced by VA-II Diode Pumped Solid State Laser (DPSS Laser, from PhotoniTech, 1.50A current) was irradiated through the cuvette. The emission fluorescence spectrum from 400nm to 700nm was recorded at a step of 1nm per second by SpectraSense software. The result is average ± SD of 4 samples.

Cell Culture: HT-29 (human colonic adenocarcinoma cell) and MCF-7 (human breast adenocarcinoma cell) cell line were kept inside the incubator (MCO-17AIC CO2 Incubator from Sanyo) with 37°C, 5% CO_2 condition. The cell lines were maintained by routinely subculturing the cells in T-25 flasks using a culture medium prepared by mixing Dulbecco's Modified Eagle Medium (DMEM, high glucose, from Sigma) with 10% fetal bovine serum (FBS, from Gibco) and 1% penicillin-streptomycin(Sigma).

Crosslinking Folic Acid with Nanoparticles: 1 ml of FA solution (1mM) in DMSO was mixed with 3 ml of NHS (15mM) and 3 ml of EDC (75mM) in DI water. 1 ml of silica/ $NaYF_4$:$Er^{3+,}$ Yb^{3+} NP solution in PBS (5mM) was added. The solution was mixed at 50 rpm overnight. The mixture was then centrifuged down at 130,000 rpm and the residue was re-suspended PBS.

Cellular Uptake of Nanoparticles: HT-29 cells were cultured in wells of the 24-well microtiter plates for 24 hours. 100µl silica/NaYF4:Er^{3+}, Yb^{3+} (2mM in PBS) was added into 1 well and FA-silica/NaYF4:Er^{3+},Yb^{3+} (2mM) solutions were added into another well. The plates were then incubated at 37°C and 5% CO_2. At the end of 24 hours, each well containing silica/NaYF4:Er^{3+}, Yb^{3+} nanoparticles and FA-silica/NaYF4:Er^{3+},Yb^{3+} nanoparticles were washed with PBS three times and imaged.

Phase contrast bright field images were obtained with ×20 objective (total magnification 200) using a Nikon inverted binocular microscope. Confocal images were obtained using a specially modified Nikon TE2000U microscope attached by a (parameters: ×40 objective, 60 µs pixel dwell, 150 µm open pinhole, gain set to 120, resolution set to 512, average of 10 counts) were obtained by Nikon D-Eclipse C1 laser scanning confocal unit attached to Nikon Eclipse TE2000-U inverted microscope. A 980nm NIR pumped diode laser was connected by a single mode NIR optical fibre to the Nikon binocular TE2000U inverted microscope with the help of engineers of EINST Technology. A special NIR water enhanced objective lens was used to obtain clearer pictures of the cells.

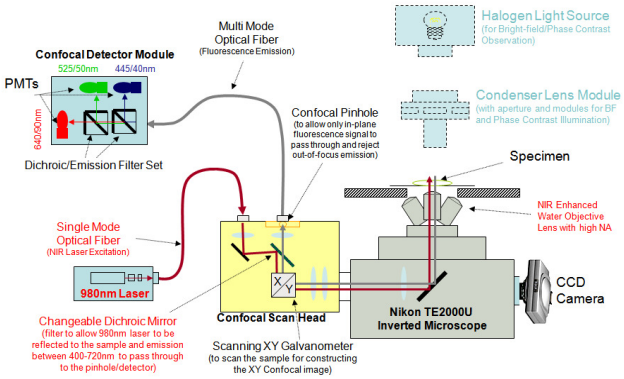

Figure 2: Schematic of the specially altered confocal microscope used for imaging of upconversion nanoparticles (the markings in red represent the changes from a standard confocal system).

3 RESULTS AND DISCUSSION

3.1 Nanoparticle characterization

Electron microscopy: The TEM pictures of the silica/$NaYF_4$:Er^{3+}, Yb^{3+} NPs are shown in Figure 3. The nanoparticles had spherical shapes and core-shell structures, with $NaYF_4$ matrix appearing as darker cores and silica coating as lighter shells. The NPs were monodisperse, having a diameter of about 30nm, with 20nm cores and 5nm thick shells. Small size and uniform size distribution facilitate the cellular uptake and are thus desired properties of nanoparticles in many biomedical applications. Smaller size also facilitates hepatic or renal removal and thus poses fewer problems in terms of biocompatibility.

The TEM image shows that the nanoparticles are aggregated. However this loose association is not the same as the solid mass that is a feature of true aggregation. The loose clustering is an artifact of the process of sample preparation whereby the drop of nanoparticle solution dried on the copper grid forces the nanoparticles to deposit in clusters when the solvent evaporates.

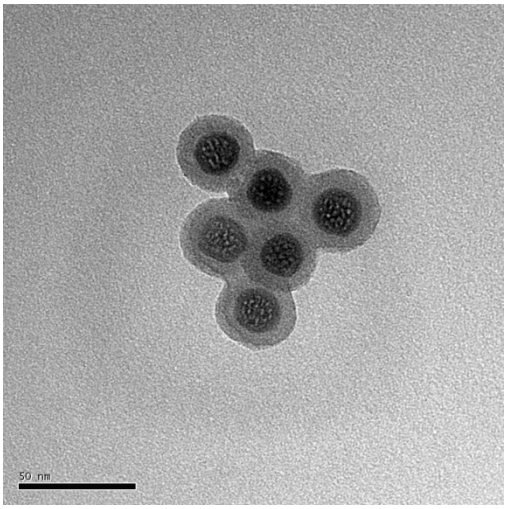

Figure 3: TEM images of silica/$NaYF_4$:Er^{3+}, Yb^{3+} nanoparticles dispersed in ethanol.

Size distribution: Figure 4 gives the size distribution graph obtained from Zetasizer. There is a single and narrow peak in the size distribution graph. 90% of the NPs fall within the range between 55nm to 110nm. The number percentage peaked at 78.8nm, and the mean diameter was calculated to be 89.9nm using the following formula:

Mean diameter = (Σ (number percentage × size))/100

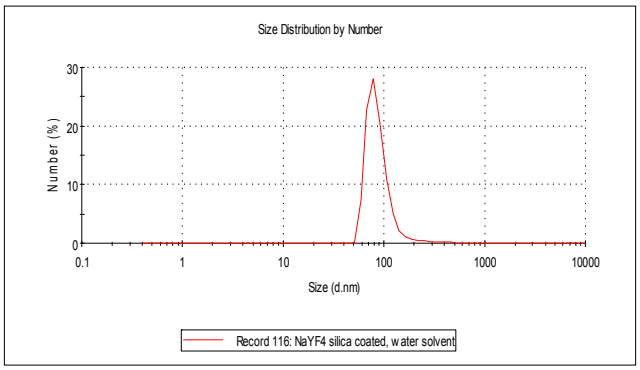

Figure 4: Size distribution by number of silica/NaYF4:Er^{3+}, Yb^{3+} nanoparticles dispersed in water at 20mM.

The single and spiky peak in the number distribution curve echoes the finding from the TEM photos that the NPs were monodisperse with narrow range of size distribution. There was no significant particle aggregation in the solution. The average size obtained by Zetasizer was considerably larger than the actual size shown in the TEM image, which can be explained by the working principle of machine. Zetasizer determines the size by measuring the Brownian motion of the particles using Dynamic Light Scattering (DLS) and correlates this information to the size of the particles. The relationship between the speed of motion and the particle size is defined in the. Because the particles are negatively charged, positive ions from the medium are attracted to the surfaces of the particles, forming a layer of liquid called the diffuse layer. This layer will move together with the particles. Therefore, the diameter of the particles given by the Zetasizer is in fact the hydrodynamic diameter instead of the actual diameter.

Emission Fluorescence: With 980nm laser input, the emission spectrum was obtained and plotted. The primary peak was observed at 541nm, with the emission count of 1085. Two secondary peaks were observed at 409nm and 656nm, with emission count of 415 and 530 respectively. The emitted light had shorter wavelength and could be used to excite photosensitizers.

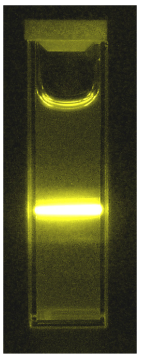

Figure 5: Visible emission on excitation with NIR laser.

Targeted uptake by cancer cells: In the case of HT-29 cells, cellular uptake was observed for both silica/$NaYF_4$:Er^{3+}, Yb^{3+} and FA- silica/$NaYF_4$:Er^{3+}, Yb^{3+} nanoparticles. However, wells containing FA-nanoparticles showed stronger and more prominent fluorescence than those incubated with unmodified nanoparticles. It suggested that the FA surface modification enhanced the targeting to HT-29 cells.

.

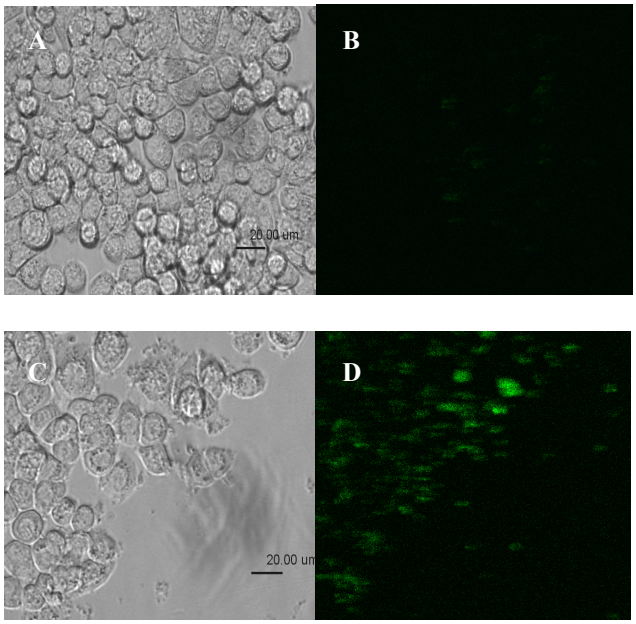

Fig 6. Bright field and confocal images of HT-29 cells incubated with UCN and FA-UCN. Bright field (A) and confocal (B) image of HT-29 cells after 24 hours of incubation showing very weak green fluorescence; corresponding bright field (C) and confocal (D) images from cells incubated with FA-UCN shows much greater take-up of the nanoparticles.

4 CONCLUSION

In conclusion, we have described the application of 30nm diameter upconversion nanoparticles for imaging of cancer cell molecular targets. The nanoparticles show little non-specific binding and almost no background fluorescence resulting in high signal-to-background ratios.

5 ACKNOWLEDGEMENT

The authors would like to acknowledge the financial support from A*STAR BMRC and National University of Singapore

REFERENCES

1. Bremer C, Tung CH, Weissleder R. In vivo molecular target assessment of matrix metalloproteinase inhibition. Nature Medicine 2001;7(6):743-748.
2. Konig K. Multiphoton microscopy in life sciences. Journal Of Microscopy-Oxford 2000;200:83-104.
3. Larson DR, Zipfel WR, Williams RM, Clark SW, Bruchez MP, Wise FW, et al. Water-soluble quantum dots for multiphoton fluorescence imaging in vivo. Science 2003;300(5624):1434-1436.
4. Zijlmans H, Bonnet J, Burton J, Kardos K, Vail T, Niedbala RS, et al. Detection of cell and tissue surface antigens using up-converting phosphors: A new reporter technology. Analytical Biochemistry 1999;267(1):30-36.
5. Niedbala RS, Feindt H, Kardos K, Vail T, Burton J, Bielska B, et al. Detection of analytes by immunoassay using up-converting phosphor technology. Anal Biochem 2001;293(1):22-30.
6. Corstjens PL, Zuiderwijk M, Nilsson M, Feindt H, Sam Niedbala R, Tanke HJ. Lateral-flow and up-converting phosphor reporters to detect single-stranded nucleic acids in a sandwich-hybridization assay. Anal Biochem 2003;312(2):191-200.
7. Lim SF, Riehn R, Ryu WS, Khanarian N, Tung CK, Tank D, et al. In vivo and scanning electron microscopy imaging of up-converting nanophosphors in Caenorhabditis elegans. Nano Lett 2006;6(2):169-74.
8. Wang F, Chatterjee DK, Li Z, Zhang Y, X. F, Wang MQ. Synthesis of polyethylenimine/NaYF4 nanoparticles with upconversion fluorescence. Nanotechnology 2006;17:5786-5791.
9. Chatterjee DK, Rufaihah AJ, Zhang Y. Upconversion fluorescence imaging of cells and small animals using lanthanide doped nanocrystals. Biomaterials 2008;29(7):937-43.